Synthesis of Aspirin-loaded Polymer−Silica Composites and their Release Characteristics

Agnieszka Kierys*

Department of Adsorption, Faculty of Chemistry, Maria Curie-Sklodowska University, M. Curie-Sklodowska Sq. 3, 20-031 Lublin, Poland

S *Supporting Information*

ABSTRACT: This study describes a novel approach to the synthesis of polymer−drug−silica nanocomposites via encapsulation/isolation of drug molecules, introduced into the polymer matrix by the silica gel. For the first time, tetraethoxysilane (TEOS) gelation in the vapor phase of the acidic catalyst is presented as an efficient method to enter the silica gel nanoparticles into the polymer−aspirin conjugate. The conducted studies reveal that the internal structure of the polymer carrier is significantly reorganized after the embedding of aspirin molecules and the silica gel. The total porosity of the polymer−drug−silica nanocomposites and the molecular structure of the silica gel embedded in the system strongly depend on the conditions of the silica source transformation. Additionally, the release of the drug was fine-tuned by adapting the conditions of hydrolysis and condensation of the silica gel precursor. Finally, to prove the usefulness of the proposed synthesis, the controlled release of aspirin from the polymer−drug−silica nanocomposites is demonstrated.

KEYWORDS: *polymer−drug−silica nanocomposite, controlled drug release, aspirin, vapor-phase synthesis, SEM*

POLYMER MATRIX   POLYMER-DRUG CUNJUGATE   POLYMER-DRUG-SILICA NANOCOMPOSITE
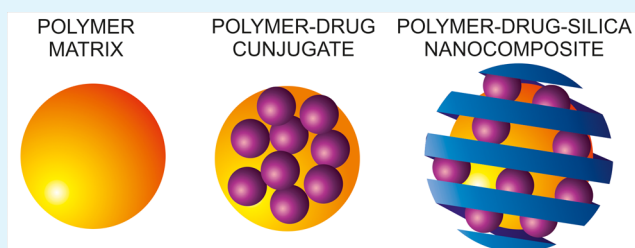
INTRODUCTION

The controlled release of pharmaceutical ingredients from delivery vehicles is not a recent development. Nonetheless, it still arouses great interest in the scientific community as well as industry. Because of the fact that the systems offering the sustained or delayed drug release from solid pharmaceutical dosage forms continue to improve, an outstanding scientific development has grown especially in the areas of materials science and biomaterials and led to an increased appreciation in medicine and pharmaceutics.

The systems of controlled release offer far-reaching advantages, namely, (i) maintenance of optimum concentration of active compounds on a therapeutic level, (ii) decrease of daily administration, (iii) matching therapy and its optimization, (iv) reduction of side effects, and (v) overcoming drug instability in biological environments.[1,2]

The design of controlled release formulations is based on a wide range of materials, both organic and inorganic, of specific properties such as biocompatibility, biodegrability, environmental sensitivity or responsiveness, sufficient mechanical resistance, and many others. One should remember that each of the delivery formulations has certain advantages as well as limitations. For example, a large group of controlled release systems has been prepared using organic carriers.[3−11] However, in many of these polymeric systems, a high initial delivery of the entrapped active agent is observed immediately upon the immersion into the released medium. Burst release is a common feature of reservoir-type and matrix, or monolithic polymeric drug delivery systems (including both swellable and

nonswellable matrices). In matrix or monolithic polymeric formulations, burst release can be ascribed to a variety of physical, chemical, and processing parameters, such as drug properties, heterogeneity of polymer matrix, synthesis conditions and storage, percolation-limited diffusion, surface characteristics of host material, host/drug interactions, morphology and porosity of dry matrix, etc.[12] Despite the fact that burst release is preferred for applications where rapid release or high initial rates of delivery may be desirable,[8,13] it is considered to be negative.[12,14,15] It is known for its properties to reduce the effective lifetime of the system and, more importantly, in the case of long-term controlled release devices, it complicates the release control of a drug and makes its administration ineffective. Moreover, burst release involves a big increase in drug concentration and, in consequence, it may even exceed the toxicity level in vivo,[15] which may induce serious adverse effects of the active ingredient. Overcoming such complication is crucial when it comes to reduction or prevention of the initial burst and achieving a constant release rate. Among the proposed solutions,[2,16,17] combining polymers of specific features with a silica gel seems to be a very interesting one. The properties that make silica nanoparticles extensively studied as an attractive host to the active agent are as follows: low toxicity, excellent biocompatibility, high surface area, tunable pore sizes, pore volumes, particles morphology

and chemical character of the silica surface.[18−23] Additionally, in 2011. the ultrasmall nonporous silica nanoparticles for targeted molecular imaging of cancer were approved for the first in-human clinical trial.[24,25] Therefore, the polymer−silica composites emerge as a promising class of materials with a notable potential addressed to many challenges pertaining to controlled drug release formulations. Recent advances have reported nanocomposites composed of cross-linked copolymer and silica gel fabricated in situ by sol−gel polymerization of the silica source under hydrolytic conditions using either acid or base catalysis.[26−28] The unique synthesis conditions of these materials make them ideal candidates for the preparation of the controlled drug release systems.[29]

The aim of this study is to present a novel approach to the polymer−drug−silica nanocomposites synthesis via encapsulation of drug molecules introduced into the polymer matrix by a silica gel. The silica gel was fabricated by gelling the silica gel precursor under an acidic vapor phase at ambient temperature. Such mild conditions of the sol−gel processes are highly appealing, particularly in the case of deposition of silica nanoparticles within a polymer network in the presence of embedded sensitive molecules such as proteins or peptides. The drug chosen for this study is aspirin due to its small molecular dimension, which allows it to enter the smallest free volumes of the polymer matrix. The hydrophilic character of this drug leads to a strong interaction with the silica gel, whose structural modeling may lead to a controllable profile release. In addition, structural differences of the polymer−drug−silica nanocomposite system prepared with a vapor-phase acid catalyst and in acidic solution are presented for comparative purposes. At this point, it should be mentioned that there are no studies on composites where the silica gel is deposited from the vapor phase on the polymer matrix with an embedded drug, as well as there are no reports on drug release from such composites, aspirin in particular. Therefore, this project provides new insights into the sustained release of aspirin from a novel polymer−drug−silica nanocomposite.

EXPERIMENTAL PROCEDURES

Materials. Amberlite XAD7HP, a nonionic aliphatic acrylic polymer of moderately polar character, was supplied by ROHM & HAAS (now Dow Chemical Co.) in the form of porous beads of well-defined porosity and used as a polymer matrix. Tetraethoxysilane (TEOS, 98%), serving as the silica source, and aspirin (ASA, acetylsalicylic acid) were supplied by Sigma-Aldrich and used as received.

Preparation of Aspirin-Loaded Nanocomposites. Initially, XAD7HP, rinsed with distilled water and dried at 80 °C under vacuum for 8 h, was immersed in an alcoholic solution of aspirin, which was already freshly prepared by dissolving aspirin in anhydrous ethanol. The aspirin solution was fully absorbed during the process of polymer swelling. Following the evaporation of the solvent at 80 °C under vacuum for 8 h, the drug-loaded polymer was labeled as P-ASA. The final concentration of aspirin was 2.5 wt % and the amount of the drug introduced was calculated on the basis of the mass balance before and after loading. First, the polymer-aspirin conjugate P-ASA was saturated with TEOS. Its amount was adjusted in such a way that the beads would stick to each other, yet preserving a loosely packed structure. After this, the vapor set P-ASA-V sample was obtained exposing the P-ASA saturated with TEOS to the vapors of 2 M HCl at autogenous pressure and room temperature for 1 day. To acquire such an effect, the freshly prepared acidic solution (10 cm³ per 1 g of P-ASA with TEOS) was poured into a sealed container. Afterward, the P-ASA beads swollen in TEOS were immediately placed over the solution and the container was tightly closed. The hydrolysis and condensation of

TEOS and SiO_2 formation took place inside the P-ASA. The P-ASA-S sample was similarly prepared, except that gelling of TEOS was performed in 2 M aqueous solution of HCl for 1 h. Then, the solid products P-ASA-S and P-ASA-V were separated, rinsed with distilled water at 10 °C, and dried at 80 °C under vacuum for 12 h. A UV−vis spectrophotometer was used to monitor the amount of aspirin that could possibly leach out during the preparation of the composite samples. Only a signal of negligible intensity was detected during the preparation of the investigated materials. Therefore, the calculated amount of the leached aspirin causes an infinitesimally small change in the total drug loading in the composites. Finally, the dry nanocomposites were hermetically sealed and stored at ambient conditions.

The amount of the silica gel contained in the samples was evaluated after the combustion of the polymer and aspirin at 650 °C for 8 h, and it was determined that the P-ASA-V sample contains about 36.65 wt % of the silica gel, whereas the P-ASA-S sample contains 28.45 wt %. The aspirin loading efficiency ranges from 25 mg/g for P-ASA to 18 mg/g for P-ASA-S and 16 mg/g for P-ASA-V, taking into account the mass of the total carrier system.

In Vitro Dissolution. The release profiles were obtained by soaking 0.2 g of the drug-loaded sample in 50 mL of 0.9% NaCl. The experiments were performed under stirring at 270 rpm at room temperature and at 36 ± 0.1 °C in a thermostated bath. For the analysis of the drug concentration, 3.0 mL of the release medium was sampled from the studied system at a predetermined time interval with the aid of UV−vis absorption spectroscopy.

Characterization Methods. The internal structure of all studied samples was verified using a scanning electron microscope (FEI Quanta 3D FEG) working at 5, 10, and 30 kV. The polymer swelling in selected solutions was studied using a Nikon SMZ1 500 stereoscopic optical microscope and automatic time-lapse imaging. The diameter and the distribution of the particles were measured with NIS-elements software using a statistical sample of about 100 objects.

The parameters characterizing the porosity of the materials were determined by the measurements of low-temperature nitrogen adsorption−desorption at −196 °C using a volumetric adsorption analyzer ASAP 2405 (Micromeritics, Norcros, GA). Prior to the experiment, all of the investigated samples were dried overnight at 80 °C under vacuum. The specific surface areas, S_{BET}, were calculated using the standard Brunauer−Emmett−Teller (BET) equation[30] for nitrogen adsorption data acquired in the range of relative pressure p/p_0 from 0.05 to 0.25. The total pore volumes, V_p, were estimated from a single point adsorption at 0.985 p/p_0. The pore size distributions (PSD) were determined from the desorption branch of the nitrogen isotherm using the Barrett−Joyner−Halenda (BJH) procedure.[31]

The molecular structure of the silica gel, condensed under different conditions, was determined using the ^{29}Si NMR spectroscopy. The solid state silicon magic-angle spinning (MAS) NMR spectra of the silica gel embedded in the polymer-drug-silica nanocomposites were obtained at resonance frequency of 59.6 MHz on a Bruker Avance 300 spectrometer. Moreover, the 4 mm zirconia rotors were used and their spin frequency was 8 kHz. About 4000 scans were applied until a satisfactory signal-to-noise ratio was achieved. The spectra were recorded using the HPDEC pulse program. The chemical shifts have been given in parts per million and referenced to tetramethylsilane as a standard material (dTMS = 0).

RESULTS AND DISCUSSION

Physicochemical Characterization of Aspirin-Loaded Composites. The presented scanning electron microscopy (SEM) micrograph (Figure 1a) reveals the complex character of the interior of XAD7HP beads employed as a matrix in the synthesis of the polymer−drug−silica nanocomposites. The method of the synthesis induced the composition of an acrylic polymer consisting of a nuclei similar in size (ca. 4.3 ± 0.5 nm). The formation of nuclei, related to polymerization, was already reported.[32,33] Nuclei create a larger structure, namely microspheres whose diameter is 45 ± 7 nm. These microspheres are
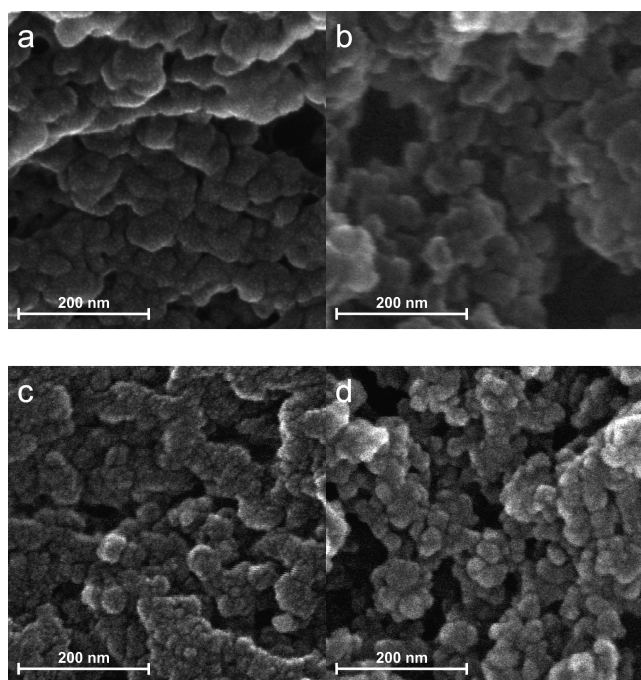
Figure 1. SEM micrographs of the pure polymer Amberlite XAD7HP (a), P-ASA (b), P-ASA-S (c), and P-ASA-V (d) (see other magnifications in the Supporting Information).

loosely connected forming an irregular continuous network of pores. The analysis of the shape of nitrogen adsorption/desorption isotherms (Figure 2) suggests a heterogeneity of the size of the pores, which is consistent with the presented micrographs. The distribution of the pore size in the pure polymer (Figure 2) is of bimodal character with peaks centered at 3.8 and 8.8 nm. The presented results may indicate that the smaller mesopores correspond to the free volumes between nuclei, whereas the bigger ones to those between microspheres.

For a quick comparison of differences between studied materials swollen in various media, the optical pictures of certain populations of wetted beads and their average diameters are collected in Table 1. The immersion of XAD7HP in the alcoholic solution of aspirin causes the polymer to swell easily and rapidly, and, as a result, the diameter of the polymer beads increases by 33%. The size of the beads after solvent evaporation decreases slightly, only by about 11%.

The SEM micrograph of the polymer—aspirin conjugate P-ASA (Figure 1b) confirms the substantial changes in its internal topography caused by the introduction of aspirin into the pore network of the polymer. The loosening of the polymer internal structure is clearly visible in Figure 1b. The changes in the

shape of N_2 adsorption/desorption isotherms and in the corresponding PSD (Figure 2a) attest the existence of the significant differences between the polymer—aspirin conjugate and the pure XAD7HP. This suggests that the internal structure of the XAD7HP polymer reorganizes during the drug solution uptake. The PSD of P-ASA is of a complex character and indicates the presence of pores within a wide range of sizes from micro- to mesopores. In addition, it is likely that the swelling in the alcoholic solution of the drug mainly influences the size of the larger free volumes in the polymer, leaving the size of the smaller mesopores, with the peak centered at 3.8 nm, almost unchanged. Moreover, the total pore volume and the specific surface area of the P-ASA are noticeably higher (Table 2).

The presented micrographs along with the parameters characterizing the porosity of the samples indicate that the aspirin molecules are mostly embedded in the free volumes between the polymer microspheres. The immersion of Amberlite XAD7HP into the alcoholic solution of the drug initiates the uptake of the molecules of both the solvent and the drug. Furthermore, because of the diffusion in the free volumes of the matrix, the inflow of the molecules is directed into the polymer interior. Because this is the cross-linked system, it is insoluble in the applied solvent. Therefore, although during the polymer swelling the internal pore network is deformed and reconstructed, the three-dimensional structure is preserved. Following the removal of ethanol, a newly formed internal pore structure is achieved. Most probably, the ASA molecules prevent the network from collapsing and they maintain the enlarged size of the beads even after the solvent evaporates. Similar mechanisms were also observed in the polymer—naproxen systems.[29] The process of aspirin precipitation during the evaporation of the solvent is considered to take place within the polymer interior, and it is unlikely that the drug is extracted to the surface. In addition, it has previously been shown that the drug concentration in the pellets loaded by swelling is higher in the center of the pellet than on its surface.[34] This might be a consequence of the drug motion together with the swollen region in the dry polymer toward the center of the matrix.[34] The absolute swelling and aging of the polymer in the used solution allow the drug molecules to freely diffuse across the entire matrix. Therefore, it can be assumed that the P-ASA composite is characterized by a homogeneous distribution of aspirin in the beads.

The release of active substances incorporated into pharmaceutical devices essentially depends on the following aspects: the specific host—guest interactions of the drug and the porosity, size, and shape of the dosage form. Accordingly, it is assumed that the introduction of the inorganic component into the polymer—aspirin conjugate may significantly change the
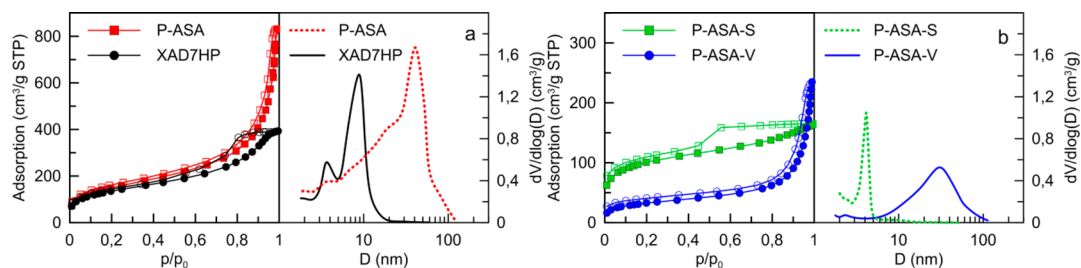

Figure 2. N_2 adsorption—desorption isotherms at standard temperature and pressure and pore size distribution of the pure polymer, XAD7HP, and P-ASA (a) and investigated composite samples (b).

Table 1. Data Obtained from the Measurements Taken with the Use of Optical Microscope
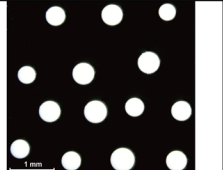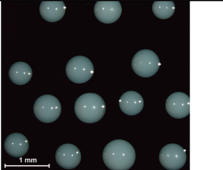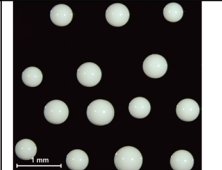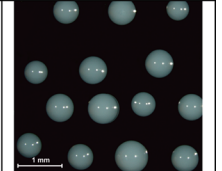
Sample	Dry polymer Amberlite XAD7HP	P-ASA immediately after swelling	P-ASA after solvent evacuation	P-ASA swollen in TEOS
Mean diameter of beads [mm]	0.48	0.64	0.57	0.62
Picture of examined sample				

Table 2. Parameters Characterizing the Porosity of the Samples Obtained from the Low Temperature N_2 Sorption[a]

sample	S_{BET} (m^2/g)	V_p (cm^3/g)	D_{p1} (nm)	D_{p2} (nm)
XAD7HP	486	0.61	3.8	8.8
P-ASA	542	1.07	3.7	40.5
P-ASA-V	118	0.30	2.3	30.2
P-ASA-S	359	0.25	4.1	

[a]S_{BET}, the specific surface area; V_p, the total pore volume; D_p, the pore diameter at the peak of PSD.

porosity and the chemical character of P-ASA and, in turn, it greatly influences the release profiles of the drug molecules. To verify these expectations, the polymer–aspirin–silica nano-composites were prepared by the introduction of the silica gel nanoparticles into P-ASA. For this purpose, the polymer–drug conjugate was saturated with the silica precursor. As it is demonstrated in Table 1, P-ASA pellets easily absorb TEOS and they swell by approximately 8%. Next, the formation of polymer–aspirin–silica composites was considered in various conditions.

The SEM micrograph in Figure 1d reveals that the vapor set P-ASA-V sample exhibits a similar internal structure to the P-ASA sample. It can be assumed that very fine silica particles, which are indistinguishable from the polymer nuclei, are formed during the condensation of the silica precursor. The nitrogen sorption results for the P-ASA-V composite are illustrated in Figure 2b. The measured N_2 adsorption–desorption isotherms are similar in shape to those of P-ASA, but the adsorption value is much lower. Adsorption and desorption isotherm branches are parallel up to the relative pressure of $p/p_0 = 0.85$ and only a very short plateau is visible at a high relative pressure. The observed hysteresis shape suggests the presence of the mainly large mesopores and the small external surface of the particles. From the analysis of the parameters characterizing the porosity (see Table 2), it follows that the specific surface area and the total pore volume of P-ASA-V are significantly smaller, compared to those in the initial materials. A possible explanation may be that the silica nanoparticles are formed in the large mesopores of the P-ASA sample, which causes the decrease of the pores' size. However, such a significant decrease of the porosity parameters may also be explained by the formation of different kinds of blockages and spatial restrictions. They can significantly limit the access of the nitrogen molecules to the free volumes or they can even close the pores. Moreover, it may be presumed that, in these particular conditions of synthesis, a specific membrane, consisting of fine SiO_2 species sticking to each other and to the pore surface of the polymer, is formed.

Previous findings show the possibility of the synthesis of highly ordered mesoporous silica films in the presence of

vapors, both the catalyst and the silica precursor or only the vapor of the silica precursor.[35,36] However, contrary to the presented system, in this preparation procedure, the starting film of the surfactant does not contain any silica precursor; it is inserted there from the vapor phase. Nevertheless, the highly ordered mesoporous silica films, presented in this work, certainly testify that the silica gel is able to form from the substrates in the vapor phase.

To compare the influence of the environment of the condensation on the composite structure, the P-ASA-S sample was synthesized by utilizing the sol–gel method in a solution. The placement of the P-ASA sample saturated with TEOS in the HCl solution causes the silica gel network to form in the polymer matrix through the reactions of polycondensation of the silica precursor. The SEM micrograph in Figure 1c reveals the complexity of the internal structure of P-ASA-S, in which rough and densely packed species of particles of different size are clearly visible.

As far as the N_2 sorption experiment is concerned, it confirms these observations. The shape of the isotherms suggests that P-ASA-S mainly contains small mesopores; the hysteresis loop is of H2 Type according to the IUPAC classification.[37] This type of hysteresis is usually attributed either to the ink-bottle shaped pores or the pores between spherically shaped elements of solids which may be interconnected. Furthermore, the emptying of the pores takes place in a very narrow range of relative pressure close to $p/p_0 = 0.5$, and, consequently, the PSD obtained by BJH method is very narrow, with a peak centered at $D_p = 4.1$ nm. However, it should be emphasized that the internal pore structure of the presented organic–inorganic system may be considered to be very complex. As a result, N_2 adsorption–desorption processes may involve, as suggested by the shape of desorption branch of the isotherm, a combination of physical mechanisms such as pore blocking and cavitation effects.[38−42] Our previous findings demonstrate that polymer–silica nanocomposites contain mesopores of various dimensions, although the steep part of the desorption branch of the isotherm is usually observed.[28,29,43]

At this point, it should be mentioned that the step on desorption isotherm is associated with the diameters of the openings of narrower pores, because their size controls the N_2 desorption process. This can be explained by the fact that during TEOS condensation, the very fine silica particles are formed of similar size as polymer nuclei. The synthesized inorganic phase is porous and occupies the mesopores. Subsequently, the specific surface area decreases slightly because of the appearance of the additional free volumes between the silica nanoparticles. The total pore volume diminishes greatly due to the presence of silica particles in the large mesopores which were originally empty in the P-ASA

14372

dx.doi.org/10.1021/am5036384 | ACS Appl. Mater. Interfaces 2014, 6, 14369−14376

sample. However, such a significant decrease of the total pore volume is probably also related to the rearrangement of the internal network of the polymer, as illustrated by SEM studies. The rearrangement of the internal network of the polymer produces a more compact structure and, consequently, eliminates large mesopores. The conclusions concerning the polymer-aspirin-silica nanocomposite are consistent with the previous studies on the polymer−silica nanocomposites in which similar gelation conditions were presented.[28,29,43]

Solid-State ^{29}Si NMR Characterization. The ^{29}Si MAS NMR spectra provide additional information concerning the chemical character of the examined nanocomposites and the form of the silica species (Figure 3). As the NMR spectra
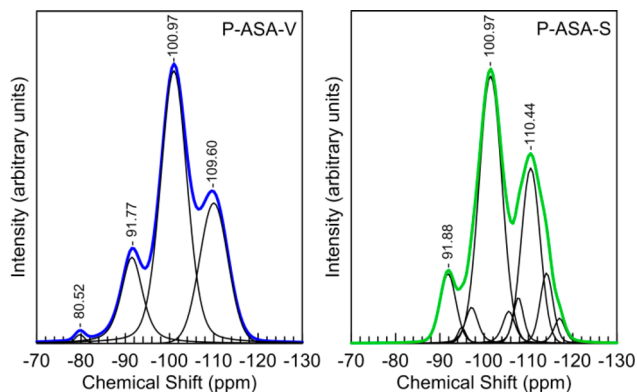

Figure 3. ^{29}Si NMR spectra of the vapor phase (P-ASA-V) and liquid set (P-ASA-S) of polymer−drug silica gels from TEOS.

indicate, there are differences in the molecular constitution of the silica gel. The spectrum of the nanocomposite fabricated in the vapor-phase acidic conditions exhibits four resonance peaks with a chemical shift of −80.52, −91.77, −100.97, and −109.60 ppm, which were identified and marked Q^1, Q^2, Q^3 and Q^4, respectively, according to the Q^n nomenclature.[44] However, only three main peaks with a chemical shift of −91.81, −100.97, and −110.44 ppm are observed for the nanocomposite synthesized in the liquid phase.

The Q^4 species representing the siloxane bridges are usually ascribed to the silica core material, whereas Q^3, Q^2 and Q^1 units

characterize the external surface of the particles. Therefore, a relative proportion of $(Q^2 + Q^3)/Q^4$, which gives information on the ratio of the silica surface to the volume of the silica skeleton, was estimated after the deconvolution of the spectra. The $(Q^2 + Q^3)/Q^4$ ratios equal 2.23 and 2.64 for P-ASA-S and P-ASA-V, respectively, and are much higher than for the silica gel synthesized by the conventional procedure, where the $(Q^2 + Q^3)/Q^4$ ratio is 0.77,[45] or for the base set polymer−silica composites.[43] The high value of this ratio suggests that the external surface of the silica species is highly developed. Hence, it can be assumed that the silica species are dispersed within the polymer−drug matrix in the form of either tiny nanoparticles or narrow threads. Furthermore, the presence of at least six additional small resonance peaks, corresponding to the detected silica species, was found in the spectrum of the P-ASA-S sample. This suggests that the silica condensates are diversely surrounded by the polymer matrix and/or the drug molecules. These observations are consistent with the previous observations (i.e., the silica gel species deeply penetrate the polymer matrix in the P-ASA-S sample).

Aspirin Release. A comparison of the aspirin release profiles for the P-ASA, P-ASA-S, and P-ASA-V nanocomposites at different temperatures is provided in Figure 4. As it follows from the desorption curves, the maximum of ~68% of aspirin is released from the P-ASA composites at room temperature. The most probable explanation of the low efficiency of the drug desorption is the low ability to swell and to expand of the polymer pore network in the aqueous solvent at room temperature. As a consequence, the drug molecules are trapped and isolated from the surroundings. A similar effect of the irreversibility of adsorption is observed in the case of gas sorption (e.g., adsorption/desorption of nitrogen) for polymer materials. It may indicate some kinetics restrictions of desorption and the presence of constriction in the pore system. The drug desorption from the polymer-aspirin system increases up to 100% when the temperature of the release medium changes from room temperature (rt) to 36 °C. Simultaneously, at this temperature, the burst release occurs in the system and almost 80% of the aspirin is being released within the first hour. The initial fast desorption of aspirin may be associated either with the morphology of the polymer matrix or with the weak
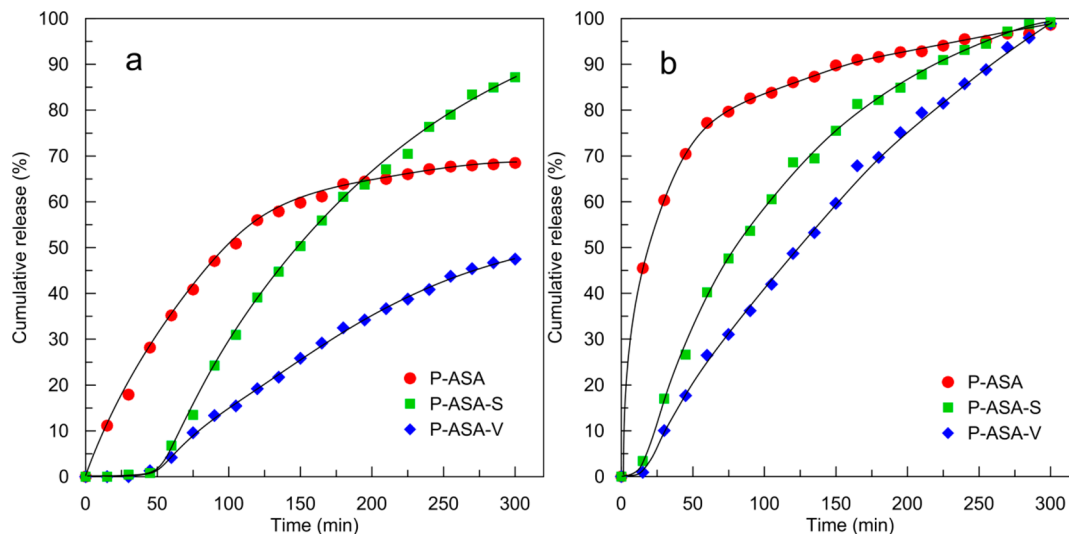

Figure 4. Aspirin release kinetics from aspirin-loaded nanocomposites. The release was measured in 0.9% NaCl solution at rt (a) and at 36 °C (b).

physical interactions between the aspirin molecules and the polymer matrix. Apart from this, the polymer pore network expands more easily at high temperature, and, as a consequence, the trapped drug molecules escape from the polymer matrix through the enlarged pores and cracks.

The desorption curves (Figure 4) clearly demonstrate that the rate of aspirin release is significantly modified by the embedding of the silica species into the P-ASA composite. First, in both silica-loaded systems (P-ASA-V and P-ASA-S), the drug release into the NaCl physiological solution is delayed either at room temperature or at 36 °C (up to 50 and 15 min, respectively). Furthermore, the degree of initial burst release is successfully diminished. Remarkably, after the lag time, both P-ASA-V and P-ASA-S samples manifest an almost linear increase of the released amount of aspirin with time. The change in the drug release rate for silica enriched systems can be mainly interpreted in terms of the chemical character of the composite carrier network.

When the hydrophobicity of the system decreases along with the incorporation of the silica into P-ASA, the specific van der Waals interactions of aspirin and silica become the main factor affecting the rate of the drug desorption. The influence of the silica content on the drug release rate of the polymer–silica composite system has already been studied and widely presented in literature. However, there are multiple opinions regarding the subject. On the one hand, it has been shown that the presence of silicates reduces the rate of drug release, and that this reduction is a function of the volume fraction of a silicate in the dexamethasone-loaded poly(ethylene-co-vinyl acetate) (EVAc) composite.[46] On the other hand, Zhong et al. have demonstrated that the aspirin release rate increases together with an increase of the content of the silica in PMMA/silica composite.[47] Thus, it can be stated that the drug release rate strongly depends on the specific interaction between the drug molecules and the component of the composites.

The preparation method of the P-ASA-V and P-ASA-S samples proves to be of crucial importance for the rate of aspirin release. Figure 4a,b presents the aspirin desorption from silica-loaded composites, collected at both rt and 36 °C. Interestingly, P-ASA-V shows similar time lag of aspirin release, compared to the P-ASA-S composite, but the efficiency of the drug desorption is much lower than in the P-ASA-S and the P-ASA composites.

The differences in the behavior of aspirin release from the silica-loaded composites can be ascribed to both the chemical character and the porosity of the composites. It should be noted that the nanocomposite fabricated in the vapor-phase conditions contains more silica gel (by 22% of weight) in comparison with the sample prepared in the liquid phase. Thus, the slower drug desorption can be attributed to the increase of the hydrophilic character resulting from the higher content of SiO_2 component. At the same time, on the basis of porosity parameters and SEM images, it can be assumed that diffusion of aspirin molecules from P-ASA-V is significantly limited. This effect may be related either to the presence of a membrane made of silica particles or to the obstruction of the transport channels occupied by the SiO_2 agglomerates.

CONCLUSIONS

The present paper has introduced a novel preparation method of the new type of the polymer–drug–silica nanocomposite and has proved its efficiency in controlled drug release systems. The conducted studies have revealed that the internal structure

of the polymer carrier is significantly reorganized after the embedding of the aspirin molecules, what seems to prevent the polymer from shrinking during the evaporation of the solvent. Additionally, TEOS gelation in the vapor phase of the acidic catalyst has been presented as an efficient method of introducing the silica gel nanoparticles into the polymer–aspirin nanocomposite. A great advantage of the vapor-phase method is the prevention of the release of the incorporated drug during TEOS gelation, which stands in contrast to the conventional sol–gel processes occurring in the solution. Moreover, the introduction of the silica gel into the polymer–aspirin conjugate modifies the chemical character and the porosity of the presented material. The total porosity of the polymer–drug–silica nanocomposites and the molecular structure of the silica gel embedded in the system strongly depend on the conditions of the transformation of the silica source. In the case of the nanocomposite obtained in the vapor-phase treatment, the tremendous decrease of the porosity parameters clearly indicates the presence of significant restrictions in the accessibility of the free volumes of the mesopores. The high value of the surface-to-volume ratio of the silica skeleton, estimated for the presented nanocomposites on the basis of ^{29}Si NMR spectra, suggests a highly developed external surface of silica species.

The embedding of the silica species in the P-ASA conjugate significantly modifies the rate of aspirin release and successfully decreases the degree of the initial burst release. It is also worth noticing that, after the lag time, the increase of the released amount of aspirin for the silica enriched systems is linear in time. Hence, the specific interaction between the drug molecules and the components of the composite play a key role in the mechanism of drug release in the composite systems. Extension of the presented experiments to other polymer–drug–silica composites is in progress and will be reported in due course.

ASSOCIATED CONTENT

Ⓢ Supporting Information

Additional SEM images of these new composites. This material is available free of charge via the Internet at http://pubs.acs.org.

AUTHOR INFORMATION

Corresponding Author

*Agnieszka Kierys. E-mail: agnieszka.kierys@umcs.lublin.pl.

Notes

The authors declare no competing financial interest.

ACKNOWLEDGMENTS

REFERENCES

(1) del Valle, E. M. M.; Galan, M. A.; Carbonell, R. G. Drug Delivery Technologies: The Way Forward in the New Decade. *Ind. Eng. Chem. Res.* **2009**, *48*, 2475−2486.

(2) Marchesan, S.; Prato, M. Nanomaterials for (Nano)medicine. *ACS Med. Chem. Lett.* **2013**, *4*, 147−149.

(3) Uhrich, K. E.; Cannizzaro, S. M.; Langer, R. S.; Shakesheff, K. M. Polymeric Systems for Controlled Drug Release. *Chem. Rev.* **1999**, *99*, 3181−3198.

(4) Peppas, N. A.; Bures, P.; Leobandung, W.; Ichikawa, H. Hydrogels in Pharmaceutical Formulations. *Eur. J. Pharm. Biopharm.* **2000**, *50*, 27−46.

(5) Freiberg, S.; Zhu, X. Polymer Microspheres for Controlled Drug Release. *Int. J. Pharm. (Amsterdam, Neth.)* **2004**, *282*, 1−18.

(6) Mora-Huertas, C. E.; Fessi, H.; Elaissari, A. Polymer-Based Nanocapsules for Drug Delivery. *Int. J. Pharm. (Amsterdam, Neth.)* **2010**, *385*, 113−142.

(7) Maderuelo, C.; Zarzuelo, A.; Lanao, J. M. Critical Factors in the Release of Drugs from Sustained Release Hydrophilic Matrices. *J. Controlled Release* **2011**, *154*, 2−19.

(8) Liu, L.; Yang, J. P.; Ju, X. J.; Xie, R.; Liu, Y. M.; Wang, W.; Zhang, J. J.; Niu, C. H.; Chu, L. Y. Monodisperse Core-shell Chitosan Microcapsules for pH-Responsive Burst Release of Hydrophobic Drugs. *Soft Matter* **2011**, *7*, 4821−4827.

(9) Vilar, G.; Tulla-Puche, J.; Albericio, F. Polymers and Drug Delivery Systems. *Curr. Drug Delivery* **2012**, *9*, 367−394.

(10) Rani, G. U.; Konreddy, A. K.; Mishra, S.; Sen, G. Synthesis and Applications of Polyacrylamide Grafted Agar as a Matrix for Controlled Drug Release of 5-ASA. *Int. J. Biol. Macromol.* **2014**, *65*, 375−382.

(11) Caballero, F.; Foradada, M.; Minarro, M.; Perez-Lozano, P.; Garcia-Montoya, E.; Tico, J. R.; Sune-Negre, J. M. Characterization of Alginate Beads Loaded with Ibuprofen Lysine Salt and Optimization of the Preparation Method. *Int. J. Pharm. (Amsterdam, Neth.)* **2014**, *460*, 181−188.

(12) Huang, X.; Brazel, C. S. On the Importance and Mechanisms of Burst Release in Matrix-Controlled Drug Delivery Systems. *J. Controlled Release* **2001**, *73*, 121−136.

(13) Mukae, K.; Bae, Y. H.; Okano, T.; Kim, S. W. A Thermosensitive Hydrogel - Poly(ethylene oxide-dimethyl siloxane-ethylene oxide) Poly(N-isopropyl acrylamide) Interpenetrating Polymer Networks. II. On-Off Regulation of Solute Release from Thermosensitive Hydrogel. *Polym. J. (Tokyo, Jpn.)* **1990**, *22*, 250−265.

(14) Park, T. G.; Cohen, S.; Langer, R. Controlled Protein Release from Polyethyleneimine-Coated Poly(L-lactic acid)/Pluronic Blend Matrices. *Pharm. Res.* **1992**, *9*, 37−39.

(15) Jeong, B.; Bae, Y. H.; Kim, S. W. Drug Release from Biodegradable Injectable Thermosensitive Hydrogel of PEG-PLGA-PEG Triblock Copolymers. *J. Controlled Release* **2000**, *63*, 155−163.

(16) Xiao, C. D.; Shen, X. C.; Tao, L. Modified Emulsion Solvent Evaporation Method for Fabricating Core-Shell Microspheres. *Int. J. Pharm. (Amsterdam, Neth.)* **2013**, *452*, 227−232.

(17) Du, P.; Liu, P. Novel Smart Yolk/Shell Polymer Microspheres as a Multiply Responsive Cargo Delivery System. *Langmuir* **2014**, *30*, 3060−3068.

(18) Kortesuo, P.; Ahola, M.; Karlsson, S.; Kangasniemi, I.; Yli-Urpo, A.; Kiesvaara, J. Silica Xerogel as an Implantable Carrier for Controlled Drug Delivery—Evaluation of Drug Distribution and Tissue Effects after Implantation. *Biomaterials* **2000**, *21*, 193−198.

(19) Radin, S.; Falaize, S.; Lee, M. H.; Ducheyne, P. In Vitro Bioactivity and Degradation Behavior of Silica Xerogels Intended as Controlled Release Materials. *Biomaterials* **2002**, *23*, 3113−3122.

(20) Gallardo, J.; Galliano, P. G.; López, J. M. P. Preparation and in Vitro Evaluation of Porous Silica Gels. *Biomaterials* **2002**, *23*, 4277−4284.

(21) Radin, S.; El-Bassyouni, G.; Vresilovic, E. J.; Schepers, E.; Ducheyne, P. In Vivo Tissue Response to Resorbable Silica Xerogels as Controlled-Release Materials. *Biomaterials* **2005**, *26*, 1043−1052.

(22) Finnie, K. S.; Waller, D. J.; Perret, F. L.; Krause-Heuer, A. M.; Lin, H. Q.; Hanna, J. V.; Barbe, C. J. Biodegradability of Sol-Gel Silica Microparticles for Drug Delivery. *J. Sol-Gel Sci. Technol.* **2009**, *49*, 12−18.

(23) Zhang, S.; Chu, Z.; Yin, C.; Zhang, C.; Lin, G.; Li, Q. Controllable Drug Release and Simultaneously Carrier Decomposition of SiO_2-Drug Composite Nanoparticles. *J. Am. Chem. Soc.* **2013**, *135*, 5709−5716.

(24) Benezra, M.; Penate-Medina, O.; Zanzonico, P. B.; Schaer, D.; Ow, H.; Burns, A.; DeStanchina, E.; Longo, V.; Herz, E.; Iyer, S.; Wolchok, J.; Larson, S. M.; Wiesner, U.; Bradbury, M. S. Multimodal Silica Nanoparticles are Effective Cancer-Targeted Probes in a Model of Human Melanoma. *J. Clin. Invest.* **2011**, *121*, 2768−2780.

(25) Bradbury, M. S.; Phillips, E.; Montero, P. H.; Cheal, S. M.; Stambuk, H.; Durack, J. C.; Sofocleous, C. T.; Meester, R. J. C.; Wiesner, U.; Patel, S. Clinically-Translated Silica Nanoparticles as Dual-Modality Cancer-Targeted Probes for Image-Guided Surgery and Interventions. *Integr. Biol.* **2013**, *5*, 74−86.

(26) Halasz, I.; Kierys, A.; Goworek, J.; Liu, H. M.; Patterson, R. E. Si-29 NMR and Raman Glimpses into the Molecular Structures of Acid and Base Set Silica Gels Obtained from TEOS and Na-Silicate. *J. Phys. Chem. C* **2011**, *115*, 24788−24799.

(27) Zaleski, R.; Kierys, A.; Grochowicz, M.; Dziadosz, M.; Goworek, J. Synthesis and Characterization of Nanostructural Polymer-Silica Composite: Positron Annihilation Lifetime Spectroscopy Study. *J. Colloid Interface Sci.* **2011**, *358*, 268−276.

(28) Zaleski, R.; Kierys, A.; Dziadosz, M.; Goworek, J.; Halasz, I. Positron Annihilation and N-2 Adsorption for Nanopore Determination in Silica-Polymer Composites. *RSC Adv.* **2012**, *2*, 3729−3734.

(29) Kierys, A.; Rawski, M.; Goworek, J. Polymer-Silica Composite as a Carrier of an Active Pharmaceutical Ingredient. *Microporous Mesoporous Mater.* **2014**, *193*, 40−46.

(30) Brunauer, S.; Emmett, P. H.; Teller, E. Adsorption of Gases in Multimolecular Layers. *J. Am. Chem. Soc.* **1938**, *60*, 309−319.

(31) Barrett, E. P.; Joyner, L. G.; Halenda, P. P. The Determination of Pore Volume and Area Distributions in Porous Substances. I. Computations from Nitrogen Isotherms. *J. Am. Chem. Soc.* **1951**, *73*, 373−380.

(32) Okay, O. Phase Separation in Free-Radical Crosslinking Copolymerization: Formation of Feterogeneous Polymer Networks. *Polymer* **1999**, *40*, 4117−4129.

(33) Gokmen, M. T.; Du Prez, F. E. Porous Polymer Particles - A Comprehensive Guide to Synthesis, Characterization, Functionalization and Applications. *Prog. Polym. Sci.* **2012**, *37*, 365−405.

(34) Forni, F.; Coppi, G.; Iannuccelli, V.; Vandelli, M. A.; Bernabei, M. T. Distribution of Drugs in Polymers Loaded by Swelling. *J. Pharm. Sci.* **1989**, *78*, 25−27.

(35) Nishiyama, N.; Tanaka, S.; Egashira, Y.; Oku, Y.; Ueyama, K. Vapor-Phase Synthesis of Mesoporous Silica Thin Films. *Chem. Mater.* **2003**, *15*, 1006−1011.

(36) Tanaka, S.; Nishiyama, N.; Oku, Y.; Egashira, Y.; Ueyama, K. Nano-Architectural Silica Thin Films with Two-Dimensionally Connected Cagelike Pores Synthesized from Vapor Phase. *J. Am. Chem. Soc.* **2004**, *126*, 4854−4858.

(37) Rouquerol, J.; Avnir, D.; Fairbridge, C. W.; Everett, D. H.; Haynes, J. M.; Pernicone, N.; Ramsay, J. D. F.; Sing, K. S. W.; Unger, K. K. Recommendations for the Characterization of Porous Solids (Technical Report). *Pure Appl. Chem.* **1994**, *66*, 1739−1758.

(38) Vishnyakov, A.; Neimark, A. V. Monte Carlo Simulation Test of Pore Blocking Effects. *Langmuir* **2003**, *19*, 3240−3247.

(39) Thommes, M. Physical Adsorption Characterization of Nanoporous Materials. *Chem. Ing. Tech.* **2010**, *82*, 1059−1073.

(40) Klomkliang, N.; Do, D. D.; Nicholson, D. On the Hysteresis Loop and Equilibrium Transition in Slit-Shaped Ink-Bottle Pores. *Adsorption* **2013**, *19*, 1273−1290.

(41) Coasne, B.; Galarneau, A.; Pellenq, R. J. M.; Di Renzo, F. Adsorption, Intrusion and Freezing in Porous Silica: The View from the Nanoscale. *Chem. Soc. Rev.* **2013**, *42*, 4141−4171.

(42) Landers, J.; Gor, G. Y.; Neimark, A. V. Density Functional Theory Methods for Characterization of Porous Materials. *Colloids Surf., A* **2013**, *437*, 3−32.

(43) Gorgol, M.; Tydda, M.; Kierys, A.; Zaleski, R. Composition of Pore Surface Investigated by Positron Annihilation Lifetime Spectroscopy. *Microporous Mesoporous Mater.* **2012**, *163*, 276−281.

(44) Engelhar, G.; Jancke, H.; Hoebbel, D.; Wieker, W. Structural Studies on Silicate Anions in Aqueous-Solution Using Si-29 NMR-Spectroscopy. *Z. Chem.* **1974**, *14*, 109−110.

(45) Fyfe, C. A.; Gobbi, G. C.; Kennedy, G. J. Quantitatively Reliable Si-29 Magic-Angle Spinning Nuclear Magnetic-Resonance Spectra of Surfaces and Surface-Immobilized Species at High-Field Using a Conventional High-Resolution Spectrometer. *J. Phys. Chem.* **1985**, *89*, 277−281.

(46) Cypes, S. H.; Saltzman, W. M.; Giannelis, E. P. Organosilicate-Polymer Drug Delivery Systems: Controlled Release and Enhanced Mechanical Properties. *J. Controlled Release* **2003**, *90*, 163−169.

(47) Lin, M.; Wang, H. T.; Meng, S.; Zhong, W.; Li, Z. L.; Cai, R.; Chen, Z.; Zhou, X. Y.; Du, Q. G. Structure and Release Behavior of PMMA/Silica Composite Drug Delivery System. *J. Pharm. Sci.* **2007**, *96*, 1518−1526.